Amphotericin B Deoxycholate in adults with Cryptococcal Meningitis; a Population Pharmacokinetic Model and Meta-Analysis of Outcomes

Katharine E Stott[a,b], Justin Beardsley[c], Sarah Whalley[a], Freddie Mukasa Kibengo[d] , Nguyen Thi Hoang Mai[e], Ruwanthi Kolamunnage-Dona[f], William Hope[a*], Jeremy Day[c,g]

[a] Antimicrobial Pharmacodynamics and Therapeutics Laboratory, Department of Molecular and Clinical Pharmacology, Institute of Translational Medicine, University of Liverpool, UK
[b] Malawi-Liverpool-Wellcome Trust Clinical Research Programme, Blantyre, Malawi
[c] Oxford University Clinical Research Unit, Ho Chi Minh City, Viet Nam
[d] MRC/UVRI Uganda Research Unit on AIDS, Entebbe, Uganda
[e] Hospital for Tropical Diseases, Ho Chi Minh City, Viet Nam
[f] Department of Biostatistics, Institute of Translational Medicine, University of Liverpool, UK
[g] Centre for Tropical Medicine and Global Health, Nuffield Department of Medicine, University of Oxford, UK
* Corresponding author: hopew@liverpool.ac.uk

Keywords: Cryptococcal meningitis, pharmacokinetics, pharmacodynamics, amphotericin B deoxycholate

ABSTRACT

There is a limited understanding of the population pharmacokinetics (PK) and pharmacodynamics (PD) of amphotericin B deoxycholate (DAmB) for cryptococcal meningitis (CM). A PK study was conducted in n=42 patients receiving DAmB 1 mg/kg q24h. A 2-compartment PK model was developed. Patient weight influenced clearance and volume in the final structural model. Monte Carlo simulations estimated drug exposure associated with various DAmB dosages. A search was conducted for trials reporting outcomes of CM patients treated with DAmB monotherapy and a meta-analysis was performed.

The PK parameter means (standard deviation) were: clearance, 0.03 (0.01) x weight + 0.95 (0.02) litres/hour; volume, 0.89 (0.90) x weight + 1.54 (1.13) litres; first-order rate constant from central to peripheral compartment, 7.12 (6.50) $hours^{-1}$; from peripheral to central compartment, 12.13 (12.50) $hours^{-1}$. The meta-analysis suggested that DAmB dosage explained most of the heterogeneity in cerebrospinal fluid (CSF) sterility, but not in mortality outcomes. Simulations of area under concentration-time curve ($AUC_{144-168}$) resulted in median (interquartile range) values 5.83 mg.h/litre (4.66-8.55), 10.16 (8.07-14.55) and 14.51 (11.48-20.42), with dosages of 0.4, 0.7 and 1.0 mg/kg q24h respectively.

DAmB PK is described adequately by a linear model that incorporates weight on clearance and volume. Inter-patient PK variability is modest and unlikely to be responsible for variability in clinical outcome. There is a discord between the impact that drug exposure has on CSF sterility and on mortality outcomes, which may be due to cerebral pathology not reflected in CSF fungal burden, in addition to clinical variables.

INTRODUCTION

Cryptococcal meningitis is a leading infectious cause of morbidity and mortality worldwide, with approximately 223,100 incident cases and 181,100 deaths annually (1). The ten-week mortality for patients receiving the current standard-of-care is 24-31% (2-5). There have been no new antifungal agents developed for use in low-to-middle income countries in the last 3 decades. Given the paucity of new agents, one important strategy for improving clinical outcomes is a better understanding and use of currently available compounds.

Amphotericin B (AmB) is a polyene antifungal agent with broad spectrum activity against yeasts and moulds, as well as some parasites. AmB was initially isolated from a streptomycete and described in 1955 (6). AmB was the first therapeutic option for treatment of lethal invasive fungal diseases such as cryptococcal meningitis (7, 8). Amphotericin B deoxycholate (DAmB) is the most potent formulation of AmB on a mg-mg basis (9, 10) and is a mainstay for the treatment of cryptococcal meningitis.

Clinical studies have progressively examined escalating dosages of 0.4mg/kg q24h (11, 12), 0.7mg/kg q24h (13-15) and 1.0mg/kg q24h (5) of DAmB for cryptococcal meningitis. The primary motivation of these studies was identification of the dosage that induces maximal antifungal activity. A regimen of 0.7 – 1.0 mg/kg q24h in combination with flucytosine for two weeks is currently recommended for induction therapy (16). Higher DAmB dosages are associated with increased rates of cerebrospinal fluid (CSF) sterilisation (2) and improved mortality (4, 5, 17). However, the broad clinical utility of DAmB is compromised by dose-limiting toxicities that include infusional reactions, phlebitis, nephrotoxicity and anaemia (18, 19). A detailed understanding of the therapeutic index for each DAmB dosage level is lacking.

Herein, we describe the development of a population pharmacokinetic model of DAmB. In addition, a meta-analysis of clinical trials of DAmB monotherapy was performed to estimate the contribution of various DAmB dosages to the observed heterogeneity in study outcomes. Finally, Monte Carlo simulations were performed to estimate the mean, median and dispersion of drug exposures that are associated with microbiological and clinical outcomes from DAmB monotherapy.

RESULTS

Demographics

A total of 42 patients (22 from Vietnam and 20 from Uganda) were recruited over an 11-month period between January and November 2016. Twenty two patients (52 %) were female. The overall median (range) age was 33 years (20 – 73 years), weight 48 kg (32 – 68 kg) and body mass index 18 kg/m^2 (12 – 25 kg/m^2), creatinine at enrolment 69 µmol/L (37 – 167 µmol/L) and estimated glomerular filtration rate using the Cockcroft Gault equation 76.7 mL/min/1.73m^2 (35.4 – 146.7 mL/min/1.73m^2). The demographic data are shown by ethnicity and overall in Table 1. There were no statistically significant differences between ethnic groups in any demographic variable.

Pharmacokinetic data

The final dataset included 282 of 312 total observations from the Vietnamese cohort and 197 of 241 total observations from the Ugandan cohort (mean 11.4 samples per patient, range 6-18). In total, 74 plasma samples were excluded because of absent information on the time PK samples were drawn. Figure 1 shows the raw plasma concentration-time profiles from study participants.

Population pharmacokinetic models

Initial exploration of structural models revealed that a two-compartment model fitted the data better than a three-compartment model. Specifically, the three-compartment structural model resulted in a more negative log likelihood value (-55.5 versus -42.8) and higher AIC (127.3 versus 101.9). Accordingly, subsequent model development was based on a two-compartment base model.

Model 1 was a standard two-compartment model without inclusion of covariates. Linear regressions of the Bayesian estimates of clearance and volume (derived from the mean population PK parameter values from Model 1) with weight and estimated glomerular filtration rate (eGFR) as covariates are presented in Figures 2a and 2b, respectively. A relationship was apparent between patient weight and both estimated clearance (slope 1.2, 95% confidence interval for estimate of slope 0.51 to 1.88, p=0.002) and estimated volume of the central compartment, (slope 1.08, 95% CI 0.05 to 2.11; p<0.001). Similarly, linear regression described a positive relationship between eGFR and estimated clearance (slope of linear regression 0.01, 95% CI for the slope 0 to 0.02, p<0.001) and volume (slope 0.67, 95% CI 0.36 to 0.98, p<0.001). These covariates were incorporated into the structural model as follows: Model 2 incorporated weight as a covariate with a linear term for clearance; Model 3 incorporated weight as a covariate with a non-linear term for clearance and Model 4 incorporated both weight and baseline renal function as covariates in the equations, with linear clearance. Population PK parameter estimates for all 4 models are shown in Table 2. There were no statistically significant differences in estimated clearance and volume from the standard model (Model 1) according to ethnicity. The mean (95% CI) clearance was 2.03 litres/h (1.69 – 2.38) and 2.24 litres/h (1.91 – 2.56) for Vietnamese and Ugandan patients, respectively; p-value 0.37. The mean (95% CI) volume was 33.55 litres (17.96 – 49.13) and 63.93 litres (40.98 – 86.88) for Vietnamese and Ugandan patients, respectively; p-value 0.09.

For all 4 two-compartment models the fit of the model to the data was acceptable. The model diagnostics are presented in Table 3. The coefficient of determination of a linear regression of observed-versus-predicted plots after the Bayesian step was 0.72, 0.74, 0.69 and 0.73 for Models 1, 2, 3 and 4, respectively. The intercept and slope approximated 0 and

1 respectively for each regression (Table 3). The mean parameter values predicted the observed values better than the medians. The measures of population bias and imprecision were comparable between the models, with bias -0.85, -0.34, -0.23 and -0.43 and imprecision 3.13, 2.97, 2.16 and 3.29 for Models 1, 2, 3 and 4 respectively. The more positive log likelihood value and lower Akaike information criterion (AIC) for Model 2 implied that the inclusion of weight as a covariate explained a portion of the observed variance.

The model that incorporated an exponential term for clearance (Model 3) decreased the log likelihood value and increased the AIC (Table 3). The inclusion of eGFR in Model 4 failed to increase the log likelihood value or reduce the AIC further. In addition, there was no statistically significant difference between Model 1 and either Model 3 or Model 4; the latter models were therefore rejected. Model 2 was chosen as the final model. Observed-versus-predicted plots for the population and Bayesian posterior values in the final model are shown in Figure 3. Figure 4 shows a visual predictive check (VPC) of the final model.

Meta-analysis of clinical outcome data

Five clinical trials that included a DAmB monotherapy arm were identified. There was one trial in which 63 patients received 0.4 mg/kg q24h (11), 3 in which a combined 208 patients received 0.7 mg/kg q24h (13-15) and 1 in which 99 patients received 1.0 mg/kg q24h (5). An additional study that reported clinical outcomes in untreated cryptococcal meningitis patients was also included. The baseline variables and clinical outcomes of these study arms are summarised in table 4. Due to the small number of studies, we were unable to adjust for baseline variables that may have had an impact on outcome measures (age, CD4 cell count, baseline level of consciousness, baseline fungal burden and baseline

cryptococcal antigenaemia). The forest plots of the dose-adjusted random effects model are shown in Figure 5. The model suggests that dose adjustment accounts for 77% of the heterogeneity in CSF sterility (p=0.007), but did not have a significant impact on the heterogeneity in either 2- or 10-week mortality outcomes (33%, p= 0.139 and 39%, p=0.092 respectively).

Monte Carlo simulations

Monte Carlo simulations (n = 5,000) were performed from the final population PK model. This enabled exploration of the consequences of the population PK variability, quantified in the final model, on plasma DAmB concentrations in a simulated population receiving the dosage regimens for which clinical trial outcome data were available. The median (interquartile range) $AUC_{144\text{-}168}$ was 5.91 mg/L*h (4.96 – 9.33 mg/L*h) for patients receiving DAmB 0.4 mg/kg q24h, 10.21 mg/L*h (8.51 – 15.72 mg/L*h) for 0.7 mg/kg q24h and 14.61 mg/L*h (12.14 – 22.03 mg/L*h) for 1.0mg/kg q24h. The $AUC_{144\text{-}168}$ distributions from the simulations are shown in Figure 6.

DISCUSSION

We conducted a PK study in HIV positive adults with cryptococcal meningitis in regions of high disease burden, and developed a population PK model that enabled the extent of interpatient variability to be quantified. We described the PK of DAmB using a 2-compartment PK model with i.v. infusion and first-order clearance of drug from the central compartment. Simulated AUCs reveal relatively modest PK variability, suggesting that the frequently poor clinical outcomes are not the result of significant PK variability. The relationship between weight and drug clearance suggests that weight accounts for a portion of the observed variance. Dosage adjustment on the basis of weight is necessary to ensure lighter patients are not over-dosed and heavier patients are not under-dosed. However, the lack of impact of either eGFR or ethnicity on the PK suggests that dosage adjustment for these variables is not necessary to achieve comparable drug exposure across patient populations.

The model-simulated median AUC of 10.17 mg.h/L following a regimen of 0.7 mg/kg q24h is consistent with AUCs estimated using non-compartmental techniques. For example, Bekersky et al calculated an AUC_{0-24} of 13.9 +/- 2 mg.h/L after 0.6 mg/kg i.v. in healthy volunteers (20). However, the simulations following 1mg/kg resulted in a median AUC of 14.52 mg.h/L, which is considerably lower than that derived from a non-compartmental analysis (NCA) conducted by Ayestarán *et al* for the same dose administered to neutropenic patients (28.98 +/- 15.46 mg.h/L) (21). The reason for this is not immediately clear but may relate to physiological differences between these two critically unwell patient cohorts (22).

Our meta-analysis of clinical outcomes from studies of DAmB monotherapy is limited by the fact that the included studies recorded CSF sterility at diverse time points ranging from 2 weeks (14) to 10 weeks (11). Nevertheless, the meta-analysis suggests that the

dosage of DAmB has a significant impact on the proportion of patients with sterile CSF and that achieving CSF sterility is dose-dependent up to 1mg/kg q24h. However, DAmB does not have a dose-dependent relationship with mortality at either 2 or 10 weeks.

The potential reasons that DAmB dosage has a positive impact on CSF sterilisation, but not mortality are as follows: first, AmB toxicity may contribute to mortality (18, 19). Nephrotoxicity is dose-dependent and likely multifactorial. It is associated with 4.5 times increase in the odds of mortality from cryptococcal meningitis at 10 weeks (18). Free drug interacts with the distal tubules of the nephron causing increased monovalent ion delivery, with consequent afferent arteriolar constriction (23). Direct tubular toxicity results in hypokalaemia and hypomagnesaemia leading to cardiotoxicity (23, 24). Conversely, rapid infusion of AmB can result in extracellular shift of potassium, causing hyperkalaemia and cardiac dysrhythmias (25). Anaemia occurs in up to 75% of patients treated with DAmB as a result of direct suppression of erythropoiesis (23). Severe anaemia more than doubles the odds of 10-week mortality from cryptococcal meningitis (18). Secondly, mortality may be driven by factors not directly resulting from either disease or treatment. For example, nosocomial bacteraemia may occur in up to 15-18% of patients hospitalised for cryptococcal meningitis (26). Third, fungal burden – and therefore conceivably, time to CSF sterility - is just one of multiple clinical variables associated with mortality in cryptococcal meningitis. Older age, altered mental status, low body weight, high peripheral white blood cell count and anaemia are independently associated with mortality at either 2 or 10 weeks (4). Immune reconstitution inflammatory syndrome (IRIS) remains a significant cause of mortality, occurring in 3-49% of cryptococcal meningitis patients surviving to initiation of antiretroviral treatment and carrying a mortality rate of up to 36% (17, 27). Raised intracranial pressure is an additional factor associated with mortality and at least 1

therapeutic lumbar puncture imparts a relative survival advantage of 69% in the first 10 days of treatment (28). Finally, the trial cohorts included in the meta-analysis were from diverse sites in Africa, Asia, Europe and the USA. Factors such as health seeking behaviour and nutritional status may have influenced mortality outcomes. Our meta-analysis did not include any baseline factors besides DAmB dosage and we are therefore unable to identify whether they account for the heterogeneity in mortality that is not explained by DAmB dosage.

The discordance between the influence that drug dosage has on CSF sterilisation and mortality is reflective of a growing consensus that CSF sterility is just one of many determinants of mortality in cryptococcal meningitis. A systematic review of 27 clinical trials determined that there was no correlation between CSF sterility at 2 weeks and all-cause mortality at either 2 or 10 weeks (29). The most biologically plausible explanation for this is that fungal burden in the CSF may not reflect the extensive encephalitis that is characteristic of cryptococcal meningitis (which is more accurately termed meningoencephalitis). Histopathological defects are more marked in patients co-infected with HIV; fungi accumulate in perivascular spaces, are deposited [predominantly extracellularly] in brain parenchyma, and form granulomatous cryptococcomas in brain tissue (30, 31). It is conceivable that brain parenchymal damage is a dominant determinant of mortality and that clearance of fungi in CSF is not mirrored by clearance in the cerebrum and other CNS subcompartments. CSF sterility is an imperfect surrogate for the extent to which drug has penetrated to and sterilised the central nervous system.

The meta-analysis suggests a strong dose-exposure-response relationship. Higher dosages are likely to be required to achieve efficacious drug exposure at the site of infection. DAmB has a large molecular weight (924 g/mol) and complex binding properties

(32). It does not readily penetrate the intact blood-brain barrier. Its concentration in meninges and cryptococcomas has been technically difficult to quantify in any finer detail than brain homogenates in preclinical models (33, 34). This challenge is compounded by a lack of clarity regarding the DAmB concentration required for therapeutic efficacy at the site of infection. Animal studies estimate that the cerebral concentration of DAmB at which the suppression of growth is half-maximal is 0.02 mg/litre in mice and 0.154 mg/litre in rabbits (33). AmB exposure above the level required to optimise antifungal activity appears only to contribute to toxicity (33, 35). Our simulations suggest that the optimal plasma AUC value in humans lies somewhere between 10-15 mg.h/L, though the information required to extrapolate this to cerebral DAmB concentrations is not currently available. The application of non-invasive, high-resolution technologies including Matrix-Assisted Lazer Desorption and Ionisation- Mass Spectroscopy Imaging (MALDI-MSI) is now possible, and offers the exciting potential to elucidate the PK/PD index associated with efficacy at the site of infection by enabling quantification of drug in specific cerebral sites, as has been demonstrated in murine models with gatifloxacin (36), doxycycline (37), pretomanid (38) and rifampicin (39).

It may be the case that the maximal antifungal effect of DAmB is achieved with a dose of approximately 0.7 mg/kg, or slightly higher, and that gains made above this dose in terms of CSF sterility are offset by losses in terms of excessive toxicity. This may explain why significant increases in the proportion of patients achieving CSF sterility are not mirrored by reductions in mortality. The present analysis is not sufficient to more precisely define the optimal dosage of DAmB. This is partly due to the lack of consensus regarding DAmB exposure targets. We are unable to propose exposure targets based on our dataset, which does not include site-specific PK or detailed toxicodynamic data. In addition, the

pharmacodynamic and clinical outcome data presented herein are derived from patient cohorts that are distinct from the patients that provided samples for the PK analysis. DAmB monotherapy at dosages of 0.7 mg/kg q24h and 1.0 mg/kg q24h has not been directly compared in a randomised controlled trial. However, comparison of these dosages in combination with 5FC has been performed. Bicanic *et al* demonstrated increased early fungicidal activity with 1mg/kg q24h DAmB versus 0.7mg/kg q24h DAmB, both in combination with 5FC 100mg/kg/day in four divided dosages, but this was not reflected in reductions in mortality. A higher percentage of deaths was seen in the higher dose DAmB arm at both 2 weeks (9% versus 3%) and 10 weeks (26% versus 21%) but this was not statistically significant (p= 0.62 and 0.77 at 2 and 10 weeks, respectively) (2).

In summary, these analyses suggest that the optimal dosage of DAmB for the treatment of cryptococcal meningitis lies between 0.7-1.0 mg/kg q24h. The precise drug exposure target that optimises clinical outcomes without producing significant toxicity remains to be defined. The extent of inter-individual PK variability in DAmB is modest and unlikely to account for the consistently poor clinical outcomes of cryptococcal meningitis.

279 MATERIALS AND METHODS

280 **Clinical Pharmacokinetic Studies**

281 Plasma samples were obtained from adults with HIV associated cryptococcal
282 meningitis. Patients were initially recruited from a multicentre randomised controlled trial
283 of adjuvant treatment with dexamethasone in HIV-associated cryptococcal meningitis
284 reported elsewhere (n=3, International Standard Registered Clinical Number 59144167)
285 (40). Following the early cessation of this trial, they were recruited from a prospective
286 descriptive study at the same sites (n=39). Patients were recruited in 2 sites: The Hospital
287 for Tropical Diseases in Ho Chi Minh City Vietnam, and Masaka General Hospital, Uganda.
288 The study protocols were approved by the relevant institutional review boards and
289 regulatory authorities at each trial site and by the Oxford University Tropical Research Ethics
290 Committee.

291 The protocol for the randomised controlled trial has been described previously (41).
292 Briefly, patients had HIV infection, a syndrome consistent with cryptococcal meningitis, and
293 laboratory evidence of cryptococcal infection. Patients who were pregnant, had renal
294 failure, had gastrointestinal bleeding, had received more than 7 days of anti-cryptococcal
295 antifungal therapy, were already taking corticosteroids, or required corticosteroid therapy
296 for co-existing conditions were excluded. The inclusion and exclusion criteria for the
297 prospective descriptive study were identical to those of the clinical trial. Patients received 1
298 mg/kg DAmB once daily by intravenous infusion over 5-6 hours, as well as 800mg
299 fluconazole per day. Two patients recruited during the clinical trial received dexamethasone
300 according to the following regimen: 0.3mg/kg/day intravenously (IV) for week 1,
301 0.2mg/kg/day IV for week 2, then orally 0.1mg/kg/day for week 3, 3mg/day week 4,
302 2mg/day week 5, 1mg/day week 6, then stop. For the first five patients enrolled, blood

samples were obtained immediately prior to intravenous DAmB infusion, and then at 1, 2, 4, 8, 12, 16, 20 and 24. The results for these patients informed a subsequent sampling strategy defined using optimal design theory such that patients were sampled pre-dose, then at 1, 2, 4, 8, 12 and 24 hours after the initiation of infusion. PK sampling occurred on treatment days 1 or 2, and 7. Whenever patients had lumbar punctures performed for other clinical indications such as raised intracranial pressure, paired plasma samples were collected for subsequent PK analysis. Therefore, additional sparse samples were taken up to 17 days after initial dosing. Quantitative fungal counts were determined for each lumbar puncture, as described previously (15).

Measurement of Amphotericin B Concentrations

Amphotericin B concentrations in plasma were measured using high-performance liquid chromatography (HPLC) with a Shimadzu Prominence HPLC system (Shimadzu, Milton Keynes, UK). Amphotericin B was extracted by protein precipitation. A total of 300 µL of methanol that contained piroxicam 2 mg/L (Sigma Aldrich, Dorset, UK) as internal standard was added to 100 µL of matrix. Samples were vortexed for 5 seconds and then centrifuged at 13,000 x g for 3 minutes.

One hundred-fifty µL of supernatant was removed and placed in a 96-well plate, to which 50 µL of water was added. A 50µL aliquot was injected onto a Kinetex 5µ XB-C18 liquid chromatography column (Phenomenex, Macclesfield, UK). Chromatographic separation was achieved using a gradient with the starting conditions of 75% A:25% B (0.1% formic acid in water as mobile phase A and 0.1% formic acid in acetonitrile as mobile phase B). Mobile phase B was increased to 80% over five minutes and then reduced to starting conditions for two minutes of equilibration. Amphotericin B and internal standard were

detected using UV detection at wavelengths of 406nm and 385nm; they eluted after 4.1 and 4.6 minutes, respectively.

The standard curve for amphotericin B encompassed the concentration range 0.05-8.0 mg/L and was constructed using blank matrix. The limit of quantitation was 0.05 mg/L. The coefficient of variation was <9.3% over the concentration range 0.05-8 mg/L. The intra- and inter-day variation was <7.9%.

Population Pharmacokinetic Modelling

A PK model was fitted to the data using the non-parametric adaptive grid (NPAG) algorithm of the program Pmetrics (42) version 1.5.0 for R statistical package 3.1.1. The data were weighted by the inverse of the estimated assay variance. Both two- and three-compartment models were tested, with zero-order intravenous input and first-order elimination from the central compartment. The two-compartment model took the following form:

a) $\frac{dX(1)}{dt} = R(1) - \left[\frac{SCL}{V} + K12\right] * X(1) + K21 * X(2)$

b) $\frac{dX(2)}{dt} = K12 * X(1) - K21 * X(2)$

c) $Y(1) = \frac{X(1)}{V}$

Where equations (a) and (b) describe the rate of change of the amount of drug (mg) in the central and the peripheral compartments, respectively. *X(1)* and *X(2)* are the amount of amphotericin B in milligrams (mg) in the central (c) and peripheral (p) compartments respectively. *R(1)* is the intravenous infusion of DAmB into the central compartment. *SCL* is the first-order clearance of drug (L/h) from the central compartment. *V* is the volume of the central compartment. *K12* and *K21* are the first-order inter-compartmental rate constants.

Equation (c) is the model output. The three-compartment model contained an additional equation to connect the third compartment to the second compartment in series:

d) $\frac{dX(3)}{dt} = K23 * X(2) - K32 * X(3)$

An initial condition was estimated to accommodate detectable drug in the first PK sample from those patients who received a dose of DAmB at an undocumented time before study enrolment. The non-zero initial conditions of *X(1)* and *X(2)* were estimated by assigning the respective parameters in the structural model (not shown in the equations above). A switch was coded whereby a parameterised estimate of the initial condition was multiplied by a binary covariate equal to 1 where the first PK sample was drawn after a dose of DAmB, or 0 where this represented a pre-dose sample.

Once the standard model was fitted (Model 1), the effects of patient weight, baseline eGFR and patient ethnicity on the PK of DAmB were investigated. Bidirectional stepwise multivariate linear regression of each subject's covariates versus the Bayesian posterior parameter values revealed a significant ($P < 0.05$) relationship between both weight and eGFR with estimated PK parameters. Univariate linear regression was employed, firstly to assess the relationship between patient weight and the Bayesian estimates for both clearance and volume. Since a positive relationship was observed between weight and both PK parameters, the population PK model was re-fitted to the data (Model 2) with incorporation of the following equations to describe (e) clearance *(SCL)*, and (f) volume *(V)*, as functions of patient weight (*Wt*):

e) $SCL = Int\_c + (Wt * Sl\_c)$

f) $V = Int\_v + (Wt * Sl\_v)$

Where *Int* is the intercept and *Sl* the slope of the linear regression describing the relationship between weight and clearance or volume, and the intercept and slope for each

of these PK parameters is parameterised separately. Thus, equation (a) of the structural model was replaced with:

a.2) $\frac{dX(1)}{dt} = R(1) - \left[\frac{Int_c + (Wt * Sl_c)}{Int_v + (Wt * Sl_v)} + K12\right] * X(1) + K21 * X(2).$

In addition, a power function was explored to describe the relationship between weight and clearance. In this model (Model 3), clearance was parameterised and scaled with weight to the exponent 0.75. This exponent has previously been demonstrated to usefully scale for size (43, 44). A linear relationship was maintained between volume and weight. Thus, in Model 3, equation (a) was replaced with:

a.3) $\frac{dX(1)}{dt} = R(1) - \left[\frac{SCL * Wt\text{^}0.75}{V * Wt} + K12\right] * X(1) + K21 * X(2).$

Univariate linear regression was similarly employed to assess the relationship between eGFR and the Bayesian estimates for clearance and volume. A weaker but nevertheless positive association was demonstrated. Consequently, a further structural model was fitted to the data (Model 4), with the following equation (g) explored to describe clearance (*SCL*):

g) $SCL = Int\_c + (Wt * Sl\_c) * (\frac{eGFR}{med_{eGFR}})$

where *eGFR* is the estimated glomerular filtration rate calculated for each patient by the Cockcroft-Gault equation and *med_eGFR* is the population median estimated glomerular filtration rate. In Model 4, equation (a) was replaced with:

a.4) $\frac{dX(1)}{dt} = R(1) - \left[\frac{Int_c + (Wt * Sl_c) * \left(\frac{eGFR}{med_{eGFR}}\right)}{Int_v + (Wt * Sl_v)} + K12\right] * X(1) + K21 * X(2).$

To explore whether there were significant differences between the model predicted PK parameters in Vietnamese and Ugandan patients, Bayesian estimates of volume of distribution and clearance from the central compartment were compared using a Mann-

Whitney test and a Student's t-test respectively. Since no significant relationship between ethnicity and DAmB PK was apparent, this variable was not incorporated in the final model.

The fit of the model to the data was assessed using a linear regression of observed-versus-predicted values before and after the Bayesian step. The coefficient of determination of the linear regression was noted in combination with the intercept and slope of the regression for each model. Model comparison was achieved through calculation of the log-likelihood value, the Akaike Information criterion (AIC), the mean weighted error (a measure of bias), and the bias-adjusted, mean weighted squared error (a measure of precision). To verify the ability of the final model to predict observed concentrations with acceptable accuracy, a visual predictive check (VPC) of the data was performed. For the VPC, the covariance matrix in Pmetrics was utilised to simulate 1000 patients administered DAmB on a mg per kg basis. Simulated weight was limited to the range observed in our clinical cohort.

Meta-analysis of clinical outcome data

The pharmacodynamic data from patients enrolled in the present clinical trial are confounded by the co-administration of fluconazole (17). Therefore, a search was performed for clinical trials of treatment for cryptococcal meningitis with at least one arm comprised of adult patients receiving DAmB monotherapy. For consistency, included trials were limited to those that recruited HIV-positive patients. Baseline clinical variables with demonstrated ability to predict patient mortality were selected a-priori and extracted from the studies; namely altered mental status, patient age and baseline CSF fungal burden (4, 29). To aid meaningful trial comparison, baseline fungal burden and baseline CSF

cryptococcal antigen titre were extrapolated from one another where they were not explicitly reported in the study, applying a correlation presented by Jarvis et al (4).

We collated a variety of clinical trial outcomes based on those that were commonly reported across trials of DAmB monotherapy: documented CSF sterility during trial follow-up, mortality at 2 weeks and, where possible, mortality at 10 weeks. Meta-analysis was performed on each outcome using a dose-adjusted random effects model to account for the baseline heterogeneity in the included studies. We included dose as a moderator variable in the model to assess the degree to which it explained heterogeneity in clinical outcome (45). The resulting mixed-effects model took the form:

$$\theta_i = \beta_0 + \beta_1 dose_i + u_i$$

where β_0 and β_1 are the model parameters intercept and dose respectively; $dose_i$ is the dose given in the ith study, assuming study-specific random effects; and $u_i \sim N(0, \tau^2)$, where τ^2 is the amount of residual heterogeneity among the true effects θ_i that is not accounted for by dose. We calculated to what extent dose as a moderator influenced the true average effect, and estimated the corresponding proportions of each outcome measure.

Monte Carlo Simulation

Monte Carlo simulations were performed in Pmetrics (42). Model 2 was used. Amphotericin B was administered on a mg/kg basis and infused over 5.5 hours. The initial condition of the central and peripheral compartment was defaulted to zero. The weight-based dosage of DAmB was converted to an absolute dosage by multiplying by the simulated patient's weight. This process served to mimic the bedside drug administration in

the original clinical trial, in which dosing was planned on a mg/kg basis but the absolute dose that was ultimately administered was determined by the patient's weight.

Drug exposure was quantified using the DAmB AUC (9, 10, 46). The simulated AUC for each patient was estimated 144 to 168 hours post therapy initiation. Simulations were performed to estimate the AUC that resulted from dosages administered in clinical trials of DAmB monotherapy for which PD measures were available – specifically, 0.4, 0.7 and 1.0mg/kg q24h (5, 11, 13-15).

Conflicts of Interest

William Hope holds or has recently held research grants with F2G, AiCuris, Astellas Pharma, Spero Therapeutics, Matinas Biosciences, Antabio, Amplyx, Allecra, Auspherix and Pfizer. He holds awards from the National Institutes of Health, Medical Research Council, National Institute of Health Research, and the European Commission (FP7 and IMI). WH has received personal fees in his capacity as a consultant for F2G, Amplyx, Ausperix, Spero Therapeutics, Medicines Company, Gilead and Basilea. WH is Medical Guideline Director for the European Society of Clinical Microbiology and Infectious Diseases, and an Ordinary Council Member for the British Society of Antimicrobial Chemotherapy.

Funding statement

Supported by the United Kingdom Department for International Development, the Wellcome Trust, and the Medical Research Council through a grant (G1100684/1) from the Joint Global Health Trials program, part of the European and Developing Countries Clinical Trials Partnership, supported by the European Union.
Katharine Stott is a Wellcome Trust Clinical PhD Fellow [203919/Z/16/Z].
Jeremy Day is a Wellcome Trust Intermediate Fellow [WT097147MA].

References

1. Rajasingham R, Smith RM, Park BJ, Jarvis JN, Govender NP, Chiller TM, Denning DW, Loyse A, Boulware DR. 2017. Global burden of disease of HIV-associated cryptococcal meningitis: an updated analysis. Lancet Infect Dis.
2. Bicanic T, Wood R, Meintjes G, Rebe K, Brouwer A, Loyse A, Bekker LG, Jaffar S, Harrison T. 2008. High-dose amphotericin B with flucytosine for the treatment of cryptococcal meningitis in HIV-infected patients: a randomized trial. Clin Infect Dis 47:123-30.
3. Jarvis JN, Meintjes G, Rebe K, Williams GN, Bicanic T, Williams A, Schutz C, Bekker LG, Wood R, Harrison TS. 2012. Adjunctive interferon-gamma immunotherapy for the treatment of HIV-associated cryptococcal meningitis: a randomized controlled trial. Aids 26:1105-13.
4. Jarvis JN, Bicanic T, Loyse A, Namarika D, Jackson A, Nussbaum JC, Longley N, Muzoora C, Phulusa J, Taseera K, Kanyembe C, Wilson D, Hosseinipour MC, Brouwer AE, Limmathurotsakul D, White N, van der Horst C, Wood R, Meintjes G, Bradley J, Jaffar S, Harrison T. 2014. Determinants of mortality in a combined cohort of 501 patients with HIV-associated Cryptococcal meningitis: implications for improving outcomes. Clin Infect Dis 58:736-45.
5. Day JN, Chau TT, Wolbers M, Mai PP, Dung NT, Mai NH, Phu NH, Nghia HD, Phong ND, Thai CQ, Thai le H, Chuong LV, Sinh DX, Duong VA, Hoang TN, Diep PT, Campbell JI, Sieu TP, Baker SG, Chau NV, Hien TT, Lalloo DG, Farrar JJ. 2013. Combination antifungal therapy for cryptococcal meningitis. N Engl J Med 368:1291-302.
6. Donovick R, Gold W, Pagano JF, Stout HA. 1955. Amphotericins A and B, antifungal antibiotics produced by a streptomycete. I. In vitro studies. Antibiot Annu 3:579-86.
7. Carton CA. 1952. Treatment of central nervous system cryptococcosis: a review and report of four cases treated with actidione. Ann Intern Med 37:123-54.
8. Mosberg WH, Jr., Arnold JG, Jr. 1950. Torulosis of the central nervous system; review of literature and report of 5 cases. Ann Intern Med 32:1153-83.
9. Andes D, Safdar N, Marchillo K, Conklin R. 2006. Pharmacokinetic-Pharmacodynamic Comparison of Amphotericin B (AMB) and Two Lipid-Associated AMB Preparations, Liposomal AMB and AMB Lipid Complex, in Murine Candidiasis Models. Antimicrobial Agents and Chemotherapy 50:674-684.
10. Lestner JM, Howard SJ, Goodwin J, Gregson L, Majithiya J, Walsh TJ, Jensen GM, Hope WW. 2010. Pharmacokinetics and pharmacodynamics of amphotericin B deoxycholate, liposomal amphotericin B, and amphotericin B lipid complex in an in vitro model of invasive pulmonary aspergillosis. Antimicrobial Agents & Chemotherapy 54:3432-41.
11. Saag MS, Powderly WG, Cloud GA, Robinson P, Grieco MH, Sharkey PK, Thompson SE, Sugar AM, Tuazon CU, Fisher JF, et al. 1992. Comparison of amphotericin B with fluconazole in the treatment of acute AIDS-associated cryptococcal meningitis. The NIAID Mycoses Study Group and the AIDS Clinical Trials Group. N Engl J Med 326:83-9.
12. Bennett JE, Dismukes WE, Duma RJ, Medoff G, Sande MA, Gallis H, Leonard J, Fields BT, Bradshaw M, Haywood H, McGee ZA, Cate TR, Cobbs CG, Warner JF, Alling DW. 1979. A Comparison of Amphotericin B Alone and Combined with Flucytosine in the Treatment of Cryptoccal Meningitis. New England Journal of Medicine 301:126-131.
13. Leenders AC, Reiss P, Portegies P, Clezy K, Hop WC, Hoy J, Borleffs JC, Allworth T, Kauffmann RH, Jones P, Kroon FP, Verbrugh HA, de Marie S. 1997. Liposomal

amphotericin B (AmBisome) compared with amphotericin B both followed by oral fluconazole in the treatment of AIDS-associated cryptococcal meningitis. AIDS 11:1463-71.

14. van der Horst CM, Saag MS, Cloud GA, Hamill RJ, Graybill JR, Sobel JD, Johnson PC, Tuazon CU, Kerkering T, Moskovitz BL, Powderly WG, Dismukes WE, Group tNIoAaIDMSGaACT. 1997. Treatment of Cryptococcal Meningitis Associated with the Acquired Immunodeficiency Syndrome. New England Journal of Medicine 337:15-21.
15. Brouwer AE, Rajanuwong A, Chierakul W, Griffin GE, Larsen RA, White NJ, Harrison TS. 2004. Combination antifungal therapies for HIV-associated cryptococcal meningitis: a randomised trial. Lancet 363:1764-7.
16. WHO. 2011. Rapid advice: Diagnosis, prevention and management of cryptococcal disease in HIV-infected adults, adolescents and children.,
17. Beardsley J, Wolbers M, Kibengo FM, Ggayi AB, Kamali A, Cuc NT, Binh TQ, Chau NV, Farrar J, Merson L, Phuong L, Thwaites G, Van Kinh N, Thuy PT, Chierakul W, Siriboon S, Thiansukhon E, Onsanit S, Supphamongkholchaikul W, Chan AK, Heyderman R, Mwinjiwa E, van Oosterhout JJ, Imran D, Basri H, Mayxay M, Dance D, Phimmasone P, Rattanavong S, Lalloo DG, Day JN, CryptoDex I. 2016. Adjunctive Dexamethasone in HIV-Associated Cryptococcal Meningitis. New England Journal of Medicine 374:542-54.
18. Bicanic T, Bottomley C, Loyse A, Brouwer AE, Muzoora C, Taseera K, Jackson A, Phulusa J, Hosseinipour MC, Van Der Horst C. 2015. Toxicity of amphotericin B deoxycholate-based induction therapy in patients with HIV-associated cryptococcal meningitis. Antimicrobial agents and chemotherapy 59:7224-7231.
19. Wingard JR, Kubilis P, Lee L, Yee G, White M, Walshe L, Bowden R, Anaissie E, Hiemenz J, Lister J. 1999. Clinical significance of nephrotoxicity in patients treated with amphotericin B for suspected or proven aspergillosis. Clin Infect Dis 29:1402-7.
20. Bekersky I, Fielding RM, Dressler DE, Lee JW, Buell DN, Walsh TJ. 2002. Pharmacokinetics, excretion, and mass balance of liposomal amphotericin B (AmBisome) and amphotericin B deoxycholate in humans. Antimicrob Agents Chemother 46:828-33.
21. Ayestarán A, López RM, Montoro JB, Estíbalez A, Pou L, Julià A, López A, Pascual B. 1996. Pharmacokinetics of conventional formulation versus fat emulsion formulation of amphotericin B in a group of patients with neutropenia. Antimicrobial Agents and Chemotherapy 40:609-12.
22. Roberts JA, Abdul-Aziz MH, Lipman J, Mouton JW, Vinks AA, Felton TW, Hope WW, Farkas A, Neely MN, Schentag JJ. 2014. Individualised antibiotic dosing for patients who are critically ill: challenges and potential solutions. The Lancet Infectious Diseases 14:498-509.
23. Laniado-Laborin R, Cabrales-Vargas MN. 2009. Amphotericin B: side effects and toxicity. Rev Iberoam Micol 26:223-7.
24. Deray G. 2002. Amphotericin B nephrotoxicity. J Antimicrob Chemother 49 Suppl 1:37-41.
25. Barcia JP. 1998. Hyperkalemia associated with rapid infusion of conventional and lipid complex formulations of amphotericin B. Pharmacotherapy 18:874-6.
26. Rajasingham R, Williams D, Meya DB, Meintjes G, Boulware DR, Scriven J. 2014. Nosocomial drug-resistant bacteremia in 2 cohorts with cryptococcal meningitis, Africa. Emerg Infect Dis 20:722-4.

27. Longley N, Harrison TS, Jarvis JN. 2013. Cryptococcal immune reconstitution inflammatory syndrome. Curr Opin Infect Dis 26:26-34.
28. Rolfes MA, Hullsiek KH, Rhein J, Nabeta HW, Taseera K, Schutz C, Musubire A, Rajasingham R, Williams DA, Thienemann F, Muzoora C, Meintjes G, Meya DB, Boulware DR. 2014. The effect of therapeutic lumbar punctures on acute mortality from cryptococcal meningitis. Clin Infect Dis 59:1607-14.
29. Montezuma-Rusca JM, Powers JH, Follmann D, Wang J, Sullivan B, Williamson PR. 2016. Early Fungicidal Activity as a Candidate Surrogate Endpoint for All-Cause Mortality in Cryptococcal Meningitis: A Systematic Review of the Evidence. PLOS ONE 11:e0159727.
30. Lee SC, Dickson DW, Casadevall A. 1996. Pathology of cryptococcal meningoencephalitis: analysis of 27 patients with pathogenetic implications. Hum Pathol 27:839-47.
31. Klock C, Cerski M, Goldani LZ. 2009. Histopathological aspects of neurocryptococcosis in HIV-infected patients: autopsy report of 45 patients. Int J Surg Pathol 17:444-8.
32. Kethireddy S, Andes D. 2007. CNS pharmacokinetics of antifungal agents. Expert opinion on drug metabolism & toxicology 3:573-581.
33. Livermore J, Howard SJ, Sharp AD, Goodwin J, Gregson L, Felton T, Schwartz JA, Walker C, Moser B, Muller W, Harrison TS, Perfect JR, Hope WW. 2014. Efficacy of an abbreviated induction regimen of amphotericin B deoxycholate for cryptococcal meningoencephalitis: 3 days of therapy is equivalent to 14 days. MBio 5:e00725-13.
34. Groll AH, Giri N, Petraitis V, Petraitiene R, Candelario M, Bacher JS, Piscitelli SC, Walsh TJ. 2000. Comparative efficacy and distribution of lipid formulations of amphotericin B in experimental Candida albicans infection of the central nervous system. J Infect Dis 182:274-82.
35. Lestner J, McEntee L, Johnson A, Livermore J, Whalley S, Schwartz J, Perfect JR, Harrison T, Hope W. 2017. Experimental Models of Short Courses of Liposomal Amphotericin B for Induction Therapy for Cryptococcal Meningitis. Antimicrob Agents Chemother.
36. Shobo A, Baijnath S, Bratkowska D, Naiker S, Somboro AM, Bester LA, Singh SD, Naicker T, Kruger HG, Govender T. 2016. MALDI MSI and LC-MS/MS: Towards preclinical determination of the neurotoxic potential of fluoroquinolones. Drug Test Anal 8:832-8.
37. Munyeza CF, Shobo A, Baijnath S, Bratkowska D, Naiker S, Bester LA, Singh SD, Maguire GE, Kruger HG, Naicker T, Govender T. 2016. Rapid and widespread distribution of doxycycline in rat brain: a mass spectrometric imaging study. Xenobiotica 46:385-92.
38. Shobo A, Bratkowska D, Baijnath S, Naiker S, Somboro AM, Bester LA, Singh SD, Naicker T, Kruger HG, Govender T. 2016. Tissue distribution of pretomanid in rat brain via mass spectrometry imaging. Xenobiotica 46:247-52.
39. Shobo A, Bratkowska D, Baijnath S, Naiker S, Bester LA, Singh SD, Maguire GE, Kruger HG, Govender T. 2015. Visualization of Time-Dependent Distribution of Rifampicin in Rat Brain Using MALDI MSI and Quantitative LCMS/MS. Assay Drug Dev Technol 13:277-84.
40. Beardsley J, Wolbers M, Kibengo FM, Ggayi AB, Kamali A, Cuc NT, Binh TQ, Chau NV, Farrar J, Merson L, Phuong L, Thwaites G, Van Kinh N, Thuy PT, Chierakul W, Siriboon S, Thiansukhon E, Onsanit S, Supphamongkholchaikul W, Chan AK, Heyderman R,

Mwinjiwa E, van Oosterhout JJ, Imran D, Basri H, Mayxay M, Dance D, Phimmasone P, Rattanavong S, Lalloo DG, Day JN. 2016. Adjunctive Dexamethasone in HIV-Associated Cryptococcal Meningitis. N Engl J Med 374:542-54.

41. Day J, Imran D, Ganiem AR, Tjahjani N, Wahyuningsih R, Adawiyah R, Dance D, Mayxay M, Newton P, Phetsouvanh R, Rattanavong S, Chan AK, Heyderman R, van Oosterhout JJ, Chierakul W, Day N, Kamali A, Kibengo F, Ruzagira E, Gray A, Lalloo DG, Beardsley J, Binh TQ, Chau TT, Chau NV, Cuc NT, Farrar J, Hien TT, Van Kinh N, Merson L, Phuong L, Tho LT, Thuy PT, Thwaites G, Wertheim H, Wolbers M. 2014. CryptoDex: a randomised, double-blind, placebo-controlled phase III trial of adjunctive dexamethasone in HIV-infected adults with cryptococcal meningitis: study protocol for a randomised control trial. Trials [Electronic Resource] 15:441.

42. Neely M, van	Guilder M, Yamada W, Schumitzky A, Jelliffe	RW. 2012. Accurate detection of outliers and subpopulations with Pmetrics, a nonparametric and parametric pharmacokinetic modeling and simulation package for R. Ther	Drug	Monit 34:467-476.

43. Hope WW, Seibel NL, Schwartz CL, Arrieta A, Flynn P, Shad A, Albano E, Keirns JJ, Buell DN, Gumbo T, Drusano GL, Walsh TJ. 2007. Population pharmacokinetics of micafungin in pediatric patients and implications for antifungal dosing. Antimicrob Agents Chemother 51:3714-9.

44. Brown JH, West GB. 2000. Scaling in biology. Oxford University Press on Demand.

45. Viechtbauer W. 2010. Conducting meta-analyses in R with the metafor package. Journal of Statistical Software 36:1-48.

46. Andes D, Stamsted T, Conklin R. 2001. Pharmacodynamics of Amphotericin B in a Neutropenic-Mouse Disseminated-Candidiasis Model. Antimicrobial Agents and Chemotherapy 45:922-926.

47. Mwaba P, Mwansa J, Chintu C, Pobee J, Scarborough M, Portsmouth S, Zumla A. 2001. Clinical presentation, natural history, and cumulative death rates of 230 adults with primary cryptococcal meningitis in Zambian AIDS patients treated under local conditions. Postgraduate Medical Journal 77:769-73.

Table 1: Patient demographics

Demographic or clinical characteristic	Vietnam	Uganda	Combined	p-value for difference between Vietnam and Uganda
Sex [a] (Male:Female)	12:10	8:12	20:22	
Age (years) [b]				
Mean	38	33	36	0.75†
Median	33	33	33	
Range	20 - 73	24 - 50	20 - 73	
Weight (kg) [c]				
Mean	47	49	48	0.21†
Median	46	49	48	
Range	32 - 68	35 - 60	32 – 68	
BMI (kg/m^2) [d]				
Mean	18	18	18	0.73$^{\Delta}$
Median	18	19	18	
Range	12 - 25	15 - 22	12 - 25	
Creatinine (µmol/L) [a]				
Mean	71	81	75	0.06†
Median	62	79	69	
Range	37 – 167	43 - 145	37 - 167	
eGFR (ml/min/1.73m^2) [e]				
Mean	90.6	79.3	84.7	0.19†
Median	89.8	73.5	76.7	
Range	35.4 – 136.1	49.8 – 146.7	35.4 – 146.7	

[a] *n* = 42
[b] *n* = 28
[c] *n* = 39
[d] *n* = 33
[e] *n* = 26

† Mann-Whitney test of significance
$^{\Delta}$ Unpaired t test of significance
BMI: Body Mass Index; eGFR: estimated Glomerular Filtration Rate, by Cockcroft-Gault equation

653 Table 2: Parameter estimates for the initial and modified two-compartment
654 pharmacokinetic models
655

Parameter and model	Mean	Median	Standard deviation
Model 1			
SCL (L/h)	2.19	2.46	0.77
Vc (L)	27.77	13.88	28.06
K12 (h^{-1})	3.84	2.16	6.57
K21 (h^{-1})	1.14	0.32	3.06
IC (mg)	10.16	2.55	9.00
Model 2			
SCL_{slope} (L/h/kg)	0.03	0.03	0.01
$SCL_{intercept}$ (L/h)	0.67	0.57	0.01
Vc_{slope} (L/kg)	0.82	0.36	0.80
$Vc_{intercept}$ (L)	1.76	1.99	1.29
K12 (h^{-1})	5.36	3.83	6.76
K21 (h^{-1})	9.92	0.46	12.27
IC (mg)	20.29	6.03	27.75
Model 3			
SCL (L/h/weight)	0.12	0.12	0.04
Vc (L/weight)	1.40	0.51	1.75
K12 (h^{-1})	1.69	0.50	4.09
K21 (h^{-1})	8.31	0.27	12.32
IC (mg)	30.10	7.87	40.56
Model 4			
SCL_{slope} (L/h)	0.01	0.01	0.01
$SCL_{intercept}$ (L/h)	1.50	1.31	0.74
Vc_{slope} (L)	1.26	0.52	1.39
$Vc_{intercept}$ (L)	1.64	0.01	2.96
K12 (h^{-1})	3.86	0.73	7.74
K21 (h^{-1})	11.24	0.40	13.44
IC (mg)	26.15	6.17	26.76

656
657 SCL: Clearance; Vc: Volume of distribution in central compartment; K12: first-order rate
658 constant from the central to peripheral compartment; K21, first-order rate constant from
659 peripheral to central compartment; IC: initial condition.

660 Table 3: Evaluation of the predictive performance of the initial and final model
661

Model	Log likelihood	Number of cycles to convergence	AIC	Population bias	Population imprecision	Linear regression of observed-predicted values for each patient		
						$R^{2,a}$	Intercept	Slope
Model 1	-56.3	1137	124.8	-0.85	3.13	0.72	0.08	0.97
Model 2	-42.8	1251	101.9	-0.34	2.97	0.74	0.01	1.01
Model 3	-102.7	577	221.7	-0.23	2.16	0.69	0.00	1.04
Model 4	-43.1	1704	102.7	-0.43	3.29	0.73	0.01	1.02

662
663 Model 2 included a linear function to scale DAmB clearance to patient weight.
664 Model 3 included a non-linear function to scale DAmB clearance to patient weight.
665 Model 4 included a function to scale DAmB clearance to patient weight and eGFR.
666 [a] Relative to the regression line fitted for the observed versus predicted values after the
667 Bayesian step.
668

669 Table 4: Clinical outcomes from trial data of DAmB monotherapy, by dosing regimen
670

DAmB regimen	Location	Number of patients	Median age	Median CD4 cell count per mm^3	Reduced LOC at baseline, no./total no (%)	Median baseline fungal burden, log_{10} CFU/ml	Baseline CSF CrAg titre, median	Documented CSF sterility, no./total no (%)	Mortality at 2 weeks, no./total no (%)	Mortality at 10 weeks, no./total no (%)	Percentage decrease haemoglobin, median (range)	Hypokalaemia	Reference
No treatment	Zambia	100	32	NR	NR	NR	NR	*0/100 (presumed)*	65/100 (65)	100/100 (100)	NR	NR	Mwaba et al, Postgrad Med J. 2001 (47)
0.4 mg/kg q24h	USA	63	37	NR	16/63 (25)	NR *≈ 4.2*	1:512*	25/63 (40)	5/63 (8)	NR; 9/63 at 12 weeks (14%)	NR	NR	Saag et al, NEJM 1992 (11)
0.7 mg/kg q24h	Thailand	16	34	9	1/16 (6)	5.63 (5.19 – 5.97)	1:512	NR	2/16 (13)	3/16 (19)	NR	NR	Brouwer et al, Lancet 2004 (15)
0.7 mg/kg q24h	Australia/ The Nether-lands	13	41	35	2/13 (15)	NR *≈ 3.9*	1:256	3/8 (37)	0/13 (0)	2/13 (15)	20 (45-5) at 10 weeks Fall in Hb >2g/dL: 2/13 (15%)	4/13 (31) <3mEg/L	Leenders et al, AIDS 1997 (13)
0.7 mg/kg q24h	USA	179	37	18	18/179 (10)	NR *≈ 4.8*	1:1024	91/179 (51)	11/202 (5)	NR	NR in consistent way	NR in consistent way	Van der Horst et al, NEJM 1997 (14)
1.0 mg/kg q24h	Vietnam	99	28	18	31/97 (32)	5.91 (5.49 – 6.48)	NR *≈1:4096*	52/99 (53)	25/99 (25)	44/99 (44)	All anaemia 62/99 (63). Grade 3-4 anaemia (<8g/dL): 46/99 (46)	All 54/99 (55). Gr 3-4 (<2.5mmol/L): 20/99 (20)	Day et al, NEJM 2013 (5)

671
672 LOC: level of consciousness; no.: number; CFU: Colony Forming Units; NR: not reported; CSF: cerebrospinal fluid; CrAg: cryptococcal antigen. NEJM : New England Journal Of
673 Medicine
674 * Reported in (14). Italic text indicates value extrapolated from available data.

Figure 1: Amphotericin B serum concentrations in 42 patients.
[SEE ATTACHED FILE Figure 1]

Patients received 1.0 mg/kg of amphotericin B deoxycholate (DAmB), infused over 5-6 hours.

Figure 2: Linear regression of the relationship between (a) patient weight and (b) estimated glomerular filtration rate and Bayesian posterior estimates for clearance and volume of distribution. Circles are Bayesian estimates from each patient. Solid line: linear regression.

(a)

[SEE ATTACHED FILE Figure2a_1]

R2=0.32. Clearance = 0.05*weight – 0.2

[SEE ATTACHED FILE Figure2a_2]

R^2=0.12. Volume = 1.08*weight – 24.8

(b)

[SEE ATTACHED FILEFigure2b_1]

R^2=0.17. Clearance = 0.01*weight + 1.03

[SEE ATTACHED FILE Figure2b_2]

R^2=0.36. Volume = 0.67*weight – 31.13

Figure 3: Scatter plots showing observed versus predicted values for the chosen population pharmacokinetic model after the Bayesian step (model 2).

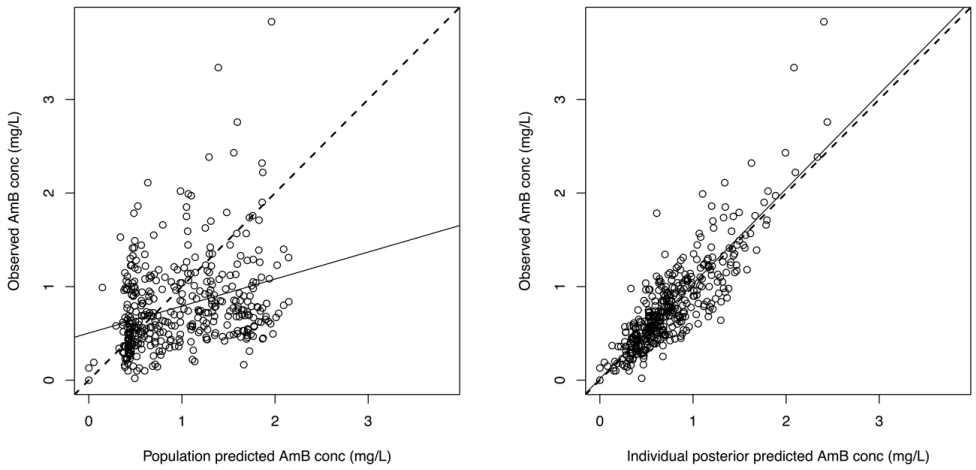

R2=0.17
Intercept = 0.18 (95% CI 0.03 – 0.32)
Slope = 0.89 (95% CI 0.70 – 1.09)

R2=0.74
Intercept = 0.01 (95% CI -0.04 – 0.07)
Slope = 1.01 (95% CI 0.95 – 1.07)

Circles, dashed lines, and solid lines represent individual observed-predicted data points, line of identity, and the linear regression of observed-predicted values, respectively. All observed and predicted amphotericin B concentrations in mg/L. AmB: Amphotericin B; CI: Confidence Interval.

Figure 4: Visual predictive check of the final model.
[SEE ATTACHED FILE Figure4.tiff]

The black circles indicate observed DAmB concentrations. The continuous lines represent the 5th, 50th and 95th percentiles of DAmB concentrations in 1000 simulated patients. In total, 83.4% of observed DAmB concentrations fall within the 5th and 95th percentiles estimated by the final model, indicating adequate model fit.

Figure 5: Meta-analysis of clinical trials of DAmB monotherapy showing dose adjusted effects on A) CSF sterility, B) Mortality at 2 weeks and C) Mortality at 10 weeks.

A)

[SEE ATTACHED FILE Figure5a.tiff]

Tau value for unadjusted model: 4.22. Tau value for dose-adjusted model: 0.98. Dose adjustment accounts for (4.22 – 0.98)/4.22 = 77% of heterogeneity in clinical outcome. P-value for dose adjustment 0.007.

B)

[SEE ATTACHED FILE Figure5b.tiff]

Tau value for unadjusted model: 1.90. Tau value for dose-adjusted model: 1.28. Dose adjustment accounts for (1.90 – 1.28)/1.90 = 33% of heterogeneity in clinical outcome. P-value for dose adjustment 0.14.

C)

[SEE ATTACHED FILE Figure5c.tiff]

Tau value for unadjusted model: 9.0. Tau value for dose-adjusted model: 4.93. Dose adjustment accounts for (9.00 – 4.93)/9.00 = 45% of heterogeneity in clinical outcome. P-value for dose adjustment 0.07.

754 Figure 6: AUC distributions based on Monte Carlo simulations

755
756
757
758
759
760
761
762
763
764
765
766 Simulated dosing regimens are 0.4, 0.7 and 1.0 mg/kg q24h. Medians, 25th and 75th percentiles displayed on each histogram (P25 and P75).